Polymer Bulletin 53, 181–192 (2005)
DOI 10.1007/s00289-004-0310-0

Polymer Bulletin

Novel Nafion/Hydroxyapatite composite membrane with high crystallinity and low methanol crossover for DMFCs

Young-Sun Park (✉), Yohtaro Yamazaki (✉)

Department of Innovative and Engineered Materials, Interdisciplinary Graduate School of Sci. and Eng., Tokyo Institute of Technology, 4259 Nagatsuta, Yokohama, 226-8502, Japan

Received: 21 October 2004 / Revised version: 28 October 2004 / Accepted: 28 October 2004
Published online: 23 December 2004

Summary

Novel Nafion/Hydroxyapatite (HA) composite membrane with high crystallinity was fabricated to suppress methanol crossover for direct methanol fuel cell (DMFC) applications. In this study, water and methanol diffusivity were evaluated through water-methanol sorption/desorption test and methanol permeation experiments. It was shown that the water-methanol diffusivity and methanol crossover for the composite membranes decrease as HA increases. Structural variation was investigated with wide-angle x-ray. As a result, it was found that the crystallinity of composite membranes increases with HA whereas water uptake content decreases gradually. Methanol permeability using a diffusion cell reduced in the composite membranes, suggesting that high crystallinity and low water uptake of composite membrane result in the suppression of methanol crossover due to the incorporation of HA into Nafion structure.

Introduction

Recently fuel cells are promising as the good alternative to conventional fossil fuels due to the protection of environment. Among the several fuel cells direct-methanol fuel cells (DMFC) are attractive particularly for a competitive portable power source; its high energy density in liquid form, inexpensiveness, and exclusion of fuel reforming process [1]. However, methanol crossover is well known to be one of the major problems blocking wide practical applications of DMFCs [2]. Methanol crossover means that supplied methanol transports through water-rich ion clusters in the Nafion® membrane from the anode to the cathode without conversion to protons by a catalytic reaction, resulting in the loss in potential, fuel consumption and thereby poor cell performance at the cathode.

Nafion® is a well-known proton-exchange polyperfluorosulfonic acid ionomer developed by E. I. Du Pont de Nemours & Co. It has been used in various fuel cells and electrochemical sensors [3,4] because of its excellent chemical stability and cation permselectivity with high ionic conductivity. Nafion® is known to be modified from polytetrafluoroethylene (PTFE) and consisted of the hydrophobic tetrafluoroethylene main chain ($-CF_2-CF_2-$) and perfluorinated vinyl ethers, terminating in the ion-

exchange sulfonic acid [5]. These sulfonic acid groups can be aggregated to form ionic clusters or ionic domains [6]. For the structural models of Nafion®, a two-phase model shows that hydrated ion clusters are embedded in the peripheral fluorocarbon medium. On the other hands, a three-phase model suggests that an interfacial region exists between the fluorocarbon matrix and ionic clusters [7]. These ion clusters seem to be interconnected through transient linked tubes of 3 - 5nm in diameter in hydrated swollen state [8].

As the origin of methanol crossover, these wide ion channels of Nafion® in the hydrated state and high hydrogen bonding energy between methanol and water have been suggested [9,10]. This large ion domains or clusters may allow easy transport of water and methanol molecules. Therefore the plasma and palladium sputtering method onto the surface of Nafion® to modify surface morphology [11,12], the fabrication of hybrid membrane using organic [13-15] and inorganic materials1 [16-23], and the fabrication of multi-layered membrane [2] have been performed to suppress methanol crossover.

In this study, we present here novel method to reduce methanol crossover using hybrid Nafion/inorganic hydroxyapatite (HA) membrane as a methanol crossover suppressant; HA shows high crystallinity more than 50%, proton-conducting property [24-26] and good compatibility with several polymers [27, 28]. We expect HA to cause structural variation within the native Nafion structure, suppressing methanol crossover.

Experimental

Materials and membrane preparation

The Nafion/HA composite membranes were fabricated using commercially available 5% Nafion solution and HA powder from Sigma-Aldrich. After HA powder was added into Nafion® solution (equivalent weight, 1100 g/mole), ultra-sonicator and magnetic stirrer were used together to mix solution homogeneously for 1 h at r.t. The homo-dispersed solutions were transparent in 2.5% and 5% Nafion/HA solutions, while milky in 7.5% solution. It was hard to find HA particles in the naked eye for all solutions, implying that the extremely homogenized solutions were fabricated. Mixed solution was poured into glass dish and remained at 70°C for 1 h on the heater plate. The cast film was detached from the glass surface by dripping distilled water, boiled in the distilled water for 1 h , cooled to r.t and then dried in vacuum at 80°C overnight.

Water and methanol diffusivity in sorption and desorption tests

We measured sorption and desorption properties of membranes for water and 2 M methanol solution at r.t. The purpose of sorption-desorption experiment is to understand the transport behavior of water or methanol molecules through the membrane only under concentration gradient. The process of sorption and desorption can be considered as the passive diffusion, i.e. without any metabolic power. On the other hands, methanol permeation using a diffusion cell can be considered to be a little fast diffusion process accompanying with some gravity or pressure effect close to real

fuel cell system. Therefore it is meaningful to understand the transport behavior of water and methanol molecules through the natural passive diffusion by sorption and desorption tests.

For water or methanol molecule to be transported through membrane, the water-methanol diffusion essentially can be preceded through the following three steps. First, methanol and water molecules should be absorbed on the surface of the membrane; second, these molecules are diffused along the ion clusters through the membrane; third, transported molecules are partitioned out of the membrane. Therefore, the sorption test involves first and second steps while the desorption test corresponds to the third step.

The dried membrane was immersed in water or 2 M methanol in a constant temperature bath at r.t. After certain time duration, the immersed membrane was taken out from the water and surface water was removed off and thereafter the weight of membrane was measured. With an increase in weight at certain time the weight gain (M_t) was obtained. The membrane was again put in the methanol solution and remained for a second time period, and the weight was re-measured. The same procedure was repeated until there was no further increase in weight and the total weight gain in water sorption (M_∞) was obtained at that time. Using the weight gains, M_t and M_∞, water sorption curve was drawn with the time, and then constant water sorption diffusivity, D_s, was obtained from the initial linear slope below about $M_t/M_\infty = 0.7$ as in eqn. (1) [29,30],

$$\frac{M_t}{M_\infty} = 4\left(\frac{Dt}{l^2}\right)^{\frac{1}{2}}\left[\frac{1}{\pi^{1/2}} + 2\sum_{n=0}^{\infty}(-1)^n \, ierfc\,\frac{nl}{2(Dt)^{1/2}}\right] \quad \textbf{(1)}$$

where D is the water diffusivity, l being the thickness of the membrane, n being an integer and ierfc X = (1/π1/2) exp (-X2) – X erfc X, where erfc X is 1-erf X and erf is the error function.

After the sorption process, water desorption process was soon proceeded from the water saturated state, i.e. M_∞ in sorption process, to dehydrated state until there is no further weight decrease, during which the weight gain M_t was obtained as like in sorption test and finally desorption diffusivity was also calculated from eqn. (1).

After the membrane was dried in vacuum at 80°C overnight, methanol sorption/ desorption experiments were proceeded as like water in 2 M methanol solution.

Transported methanol by a diffusion cell

After drying membranes in vacuum at 80°C overnight, methanol permeation measurement was proceeded like reported elsewhere [11,13,15,23] where the permeation cell consists of two compartments – one side of the permeation cell filled with methanol solution of 1.5 M, 3 M and 5 M (V = 40 ml) and the other side filled water distillated water. The water-methanol molecules diffuse through the membrane, held by bolt-nut clamp and silicon O-ring with the diameter of 20 mm and the thickness of 3mm, into the right compartment of the permeation cell, filled with the distilled water (V = 10 ml) and agitated by two magnetic stirrers. The sample solution was taken from the right compartment periodically with a micro-syringe and analyzed by capillary gas chromatography (Shimadzu GC-8AIT) at various times. A constant

helium flow, adjusted by a mass-flow controller (MFC), swept the water and methanol gas molecules into the thermal conductivity detector (TCD) of a gas chromatograph. The concentration of methanol in the right compartment linearly increases with time. The transported amount of methanol was obtained by comparing the area ratio of methanol peak at about 1.3 min and water peak at about 0.8 min with the area ratio in calibration line obtained under the methanol concentration between 1 mM and 8 M. The rate of methanol transport (J) was calculated by eqn. (2).

$$J(mmole/hr/cm^2) = \frac{1}{A} \times \frac{(c_o - c_i)}{\Delta t} \quad (2)$$

And the permeability (P) was defined by

$$P(cm/\sec) = \frac{Slope}{A} \frac{1}{(c_o - c_i)} \quad (3)$$

where C is the concentration of methanol, A being the surface area of membrane.

The methanol permeability was evaluated from the slope of the linear line of transported methanol concentration (mM) vs. permeation time (min).

Crystallinity evaluation by using wide-angle X-Ray diffractogram

The purpose of wide-angle x-ray diffraction (WAXD) is to investigate the relation between the structural changes such as crystallinity and formation of new crystalline and methanol crossover. In the crystalline and partially crystalline polymer, the periodic repeating crystalline layer gives rise to well defined sharp diffraction peaks. On the other hand, non-crystalline or amorphous material generates broad peaks. Crystallinity was evaluated quantitatively here for the cast Nafion and composite membranes and investigated the incorporation effect of HA.
X-ray specimen was prepared by allowing reserved hydrated membranes to be dried in a vacuumed drying oven at 80°C overnight. X-ray diffractogram was recorded with a Rigaku 1200 diffractometer and RINT 2000 goniometer using nickel filtered copper radiation (λ= 0.1542nm). The X-ray unit was operated at 40 kV and 20 mA. Angular scanning was continued in the range of $10° < 2\theta < 50°$ at the rate of 2 °/min. The crystallinity, X_{cr}, can be defined in eqn. (4) by rationing the integrated intensities of the separated crystalline diffraction peaks to the sum of the integrated crystalline and amorphous contributions for the decomposed diffractogram.

$$X_{cr}(\%) = \int_{10}^{22} I_{cr}(s) s^2 ds \Big/ \int_{10}^{22} [I_{cr}(s) + I_{am}(s)] s^2 ds \quad (4)$$

where I_{cr} and I_{am} are the diffracted intensities of the crystalline and amorphous peak, respectively.

Crystalline and amorphous areas were obtained through peak deconvolution process using Gaussian function [3,31-33].

Water uptake property for cast Nafion and composite membrane

The purpose of measuring water uptake content is to investigate the relation with crystallinity. It is based on the assumption: water occupies only in the amorphous region within the membrane. The dehydrated cast Nafion and composite membranes were soaked in distillated water at r.t for 1 week, referred to fully hydrated state membranes. The weight of fully hydrated membranes was measured using high precision weight balance after removing surface water with the tissue. Measured membrane was reserved again in the desiccator at r.t and the variation of weight with time was monitored. The water uptake content is given by eqn. (5):

$$Water\,uptake\ content\,(\%) = W_{hydrated} - W_{dehydrated} = \frac{W_{wet} - W_{dry}}{W_{wet}} \times 100 \quad (5)$$

where $W_{hydrated}$ and $W_{dehydrated}$ are the weights of hydrated and dehydrated membranes.

Results and discussion

Microscopy by SEM and TEM

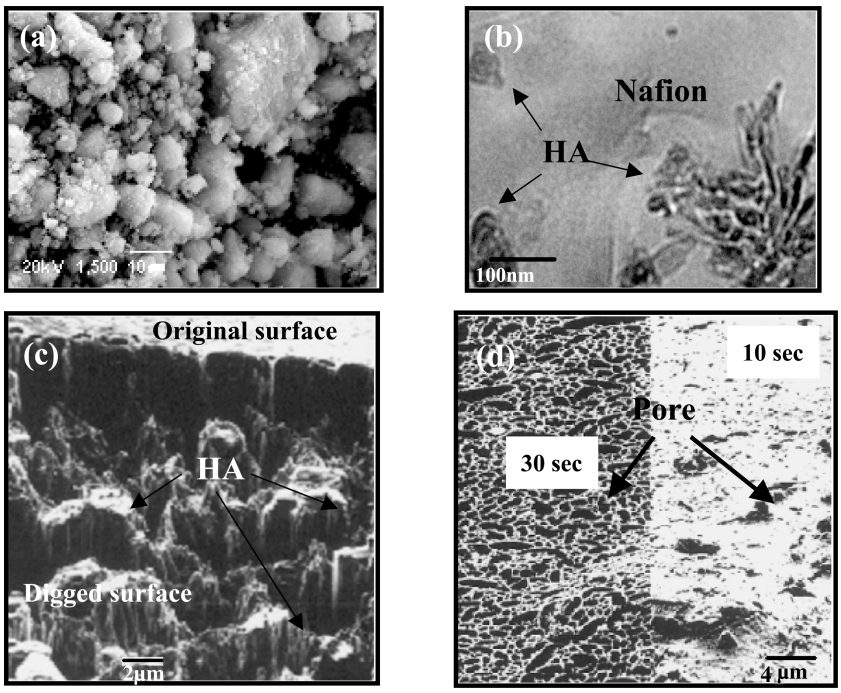

Fig. 1 Microstructure of HA (SEM, (a)), HA particle and the interface between Nafion and HA (TEM, (b)), and the distribution of HA in focused ion beam (FIB, (c)) and surface pores (FIB, (d)) at 10 and 30 sec. after Ga irradiation for 5% Nafion/HA composite membranes.

Scanning electron microscope (SEM) was used to observe the structural characteristics of HA powders. SEM micrographs of HA powder is shown in Fig. 1 (top) where a lot of agglomerates in spherical shapes are shown. It is likely that these soft agglomerates can be easily pulverized into small fragments in the homogenizing process using two sonicators. The size of HA agglomerates ranges from sub-micron to over 20 μm with a relatively broad distribution.
In Fig. 1 (bottom) transmission electron microscopy (TEM) shows that HA particles are well distributed within Nafion structure and look like a bunch of needle-like agglomerate in the range 100 - 250 nm. This aggregate seems to be consisted of many chopped fiber-like fragments. De-lamination in the interfacial region between HA and Nafion is not shown, indicating that these two materials are compatible and have strong interfacial adhesion. It is noteworthy that the size of HA aggregates decreased to 250 nm after homogenizing process, compared to over 20μm in SEM. It implies that this aggregate may be well smashed into fine fragments during the homogenizing process.

Water/Methanol sorption-desorption diffusivity

Diffusion property in water and 2 M methanol solution was investigated using sorption and desorption experiments at RT. Fig. 2 shows the sorption (a) and desorption plots (b) in the 2 M methanol for Nafion®117, cast Nafion, and composite membranes. It is shown that methanol uptake increases with time in the sorption curves while decreasing in the desorption curves. Diffusivities of sorption (D_s) and desorption (D_{ds}) were evaluated from the initial slope of the plots, below $M_t/M_\infty = 0.7$ in sorption and in the range of 0.2 – 0.8 in desorption, by setting the second term in the bracket equal to zero in eqn (2) [34-37]. The obtained total diffusivities in water and 2 M methanol are listed in table 1 where composite membranes show lower diffusivities of sorption and desorption in water and 2 M methanol. Note that water diffusivity in sorption and desorption are slightly lower than that in 2M methanol regarding the slope. The decrease in the diffusivity of water for the Nafion membrane may be based on the slow kinetic of water absorption at the membrane surface [38].

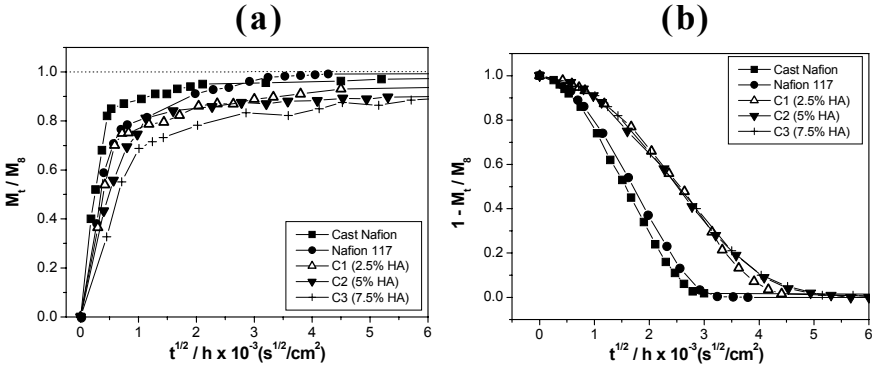

Fig. 2. Plots of 2M methanol sorption (a) and desorption (b). The slope of sorption and desorption also decreases gradually in the composite membranes as like in water sorption-desorption plots.

Table 1. The sorption (D_s), desorption (D_{ds}) and average (D_{av}) diffusivity in water and 2 M methanol at r.t using eqn. (1).

($\times 10^7$ cm^2/s)

	C/Nafion	Nafion®117	C1	C2	C3
HA (%)	-	-	2.5	5	7.5
Thickness (μm)	120	195	123	118	125
Water					
D_s	3.9	1.8	1.7	1.4	1.0
D_{ds}	0.5	0.3	0.2	0.2	0.1
D_{av}	2.2	1.2	0.9	0.8	0.6
Methanol					
D_s	7.0	3.3	2.9	1.5	1.0
D_{ds}	0.4	0.4	0.2	0.2	0.1
D_{av}	3.6	1.9	1.6	0.9	0.6

D_s: the sorption permeability, D_{ds}: the desorption permeability, D_{av}: the average permeability

Considering that the molecular size of methanol (0.13 nm) is larger than water (0.08 nm), higher diffusivity in methanol compared to water is due to high swelling by the incorporation of methanol into cluster region of membranes. Lower diffusivity in composite membranes is due to the incorporation of HA in Nafion. Comparing diffusivity in sorption with that of desorption, the former is higher than the latter, indicating the diffusion rate from liquid medium to inner membrane (sorption process) may be faster than from inner membrane to the air (desorption). The partition coefficient ($K_i = a_{i,p}/a_{i,l}$), determined from a plot of mole fractions in the liquid phase and in the polymer phase [39], is close to one, indicating that that saturated Nafion membranes shows no preference for either methanol or water [40]. It implies that the rate of sorption and diffusion may be faster than that in desorption process. The water diffusivity of 1.8 and 3.9 $\times$ 10^{-7} cm^2/s for Nafion®117 and cast Nafion is a little lower than that of the reference for Nafion® at 30°C given as 7×10^{-6} cm^{2}s^{-1} [41]. It may be due to the temperature dependence of 10°C.

The rate of methanol transport and methanol permeability

The rate of methanol flux and methanol permeability in 1.5, 3, and 5 M methanol solution were obtained using eqn. (2) and eqn. (3) in Fig. 3 and Fig. 4. Assuming methanol flux of cast Nafion in 1.5M methanol as 100%, it decreases to 85 %, 76 %, 65 % and 58 % for the Nafion®115, Nafion®117, C1 (2,5% HA), and C2 (5 % HA) composite membranes whereas 80 %, 101 %, 73 % and 63 % in order at 5 M methanol, which shows higher sensitivity of Nafion®115 at high concentration of methanol. The stationary methanol permeability as shown in Fig. 4 also decreases in composite membranes. Table 2 shows the transported methanol, methanol flux, and methanol permeability at 1.5 M, 3 M, and 5 M methanol solution. The methanol crossover difference between Nafion®117, Nafion®115, and cast Nafion may be due to the thickness gap and the structural variation between cast process and die casting

process. The composite membranes display relative lower transported methanol, methanol flux, and methanol permeability than in Nafion®117, Nafion® 115 and cast Nafion, which is possibly due to the difference in microstructure between three types of Nafion and composite membranes such as reduction in amorphous free volume of

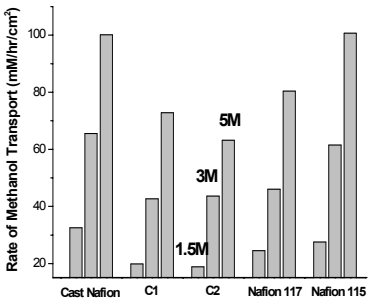

Fig. 3. Rate of methanol permeability. It is shown that permeability decreases in the composite membranes.

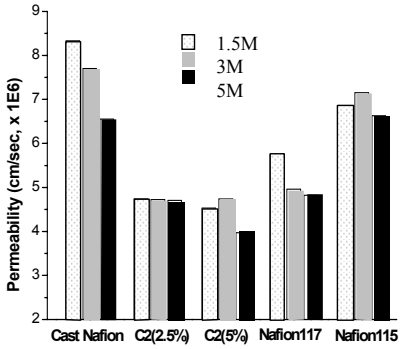

Fig. 4. Methanol permeability for Nafion®117, Nafion®115, cast Nafion, C1 (HA 2.5%), and C2 (HA 5%) Nafion/HA composite membranes in 1.5, 3 and 5M methanol solution.

clusters. Micro-dispersed embedded HA can occupy the amorphous free volume which was originally occupied by water and methanol in Nafion, resulting in the decrease of channel size and lowering the percent sorption capacity of solvent and methanol crossover as reported in Table 1 and Table 2. This low methanol crossover property in the composite membranes seems to be related to the structural change due to the incorporation of HA into Nafion structure. Crystallinity was evaluated to investigate structural variation using wide X-ray diffraction.

Crystallinity evaluation for cast Nafion and composite membrane

X-ray diffraction and peak deconvolution

Fig. 5 illustrates X-ray diffraction spectra for a series of membranes from 10° to 50° of 2θ. It is shown that the peak position of PTFE at 18.2° shifts 17.7° in cast Nafion due to the incorporation of the perfluorinated sulfonate side groups. The broad peak ranging from 30° to 50° in cast Nafion is believed to be the tiny crystalline or amorphous regions in PTFE [42]. It is noteworthy that the new crystalline peak (●), corresponding to the crystalline peak of HA, appears in this amorphous region of cast Nafion in the range 30° - 50° of 2θ. It indicates that the HA crystallite seems to be newly formed in the amorphous structure of cast Nafion in composite membranes, suggesting that HA may cause structure modification such as size of ionic cluster and the number of ionic cluster. Another new crystalline peaks (Fig. 5(b), (■)) different from HA appear in the range of 10°-16° of 2θ corresponding to amorphous region of Nafion. It indicates that new type crystallites can be created in the amorphous region of Nafion or possibly at the interface of HA and Nafion. It has been suggested that

Table 2. Transported methanol, methanol flux, and methanol permeability at 1.5, 3, and 5 M methanol at 18°C for cast Nafion, Nafion®117, Nafion®115, 2.5% and 5% Nafion/HA composite membranes.

		C/Nafion	Nafion117	Nafion115	C1(2.5%)	C2(5%)
HA (%)		-	-	-	2.5	5.0
Swelled thickness (μm)		195	206	135	200	205
Transported	1.5 M	196	148	166	119	114
Methanol	3 M	395	277	370	257	263
(mM)	5 M	602	484	606	438	380
Methanol	1.5 M	32	25	28	20	19
Flux	3 M	66	46	62	43	43
(mM/hr/cm2)	5 M	100	80	101	73	63
Methanol	1.5 M	8.3	5.7	6.8	4.7	4.5
Permeability	3 M	7.7	5.0	7.1	4.7	4.7
($\times 10^7$, cm/s)	5 M	6.6	4.8	6.6	4.7	4.0

strong polymer/filler interaction can promote a different crystallization and form a different crystalline structure or crystalline morphology. By contrast in the case of weak interface strength between polymer and inorganic material the inorganic layers disrupt the crystalline morphology. Thereby the strong interaction of Nafion/HA and successful crystallization of HA may explain the formation of new crystalline peak resulting from the structural modification. In Fig. 5(b), it is shown that the peak positions shift to the lower diffraction angles as HA increases, relating to the changes of crystalline size. The crystalline size can be calculated by the Scherrer equation in eqn. (6) [43].

$$\text{Crystallite Size} = K \times \lambda / FW \times \cos\theta \qquad (6)$$

where K is the shape factor of the average crystallite, normally 0.9, λ is the x-ray wavelength, usually 0.154056 nm for Cu Kα1, and θ is the peak position.

Table 3. Crystallinity and water uptake contents for PTFE, cast Nafion, C1, C2 and C3 composite membranes.

	PTFE	cast Nafion	C1	C2	C3
HA (%)			2.5	5.0	7.5
Avg. Crystallinity (X_{cr}, %)	64	28	31.5	36	38
Standard deviation (%)	1.6	1.5	2.6	1.7	2.1
Water uptake content (%)	-	31	26	21	18

Consequently, the calculated crystallite sizes were 4.7, 4.0, 3.7, and 3.6 nm for cast Nafion and 2.5%, 5%, 7.5% composite membranes.
Gierke et al. have noted that the crystallinity of Nafion® was in the range from 0% to 40%, calculated from the relative intensity of the amorphous halo and crystalline peak [9], possibly subtracting the instrumental background profile from the original profile. On the other hand, the crystallinity was reported in the range of 12 - 23% for Nafion-SO_2Cl and Nafion-COOH in four equivalent weights of membrane [3]. In this study, the crystallinity in the composite membranes increases as the HA increases, compared to the cast Nafion (Table 3). This increase in crystallinity has also been reported in the hybrid Nafion/silica membrane [44,45] and PEEK/HA membrane [46] as well as Nafion/HA composite membrane.

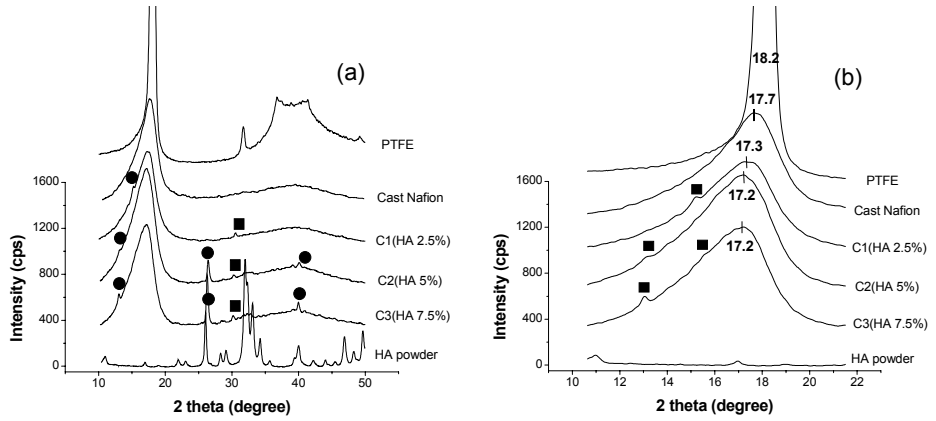

Fig. 5. New peak formation from HA (●) and from the structural modification (■) in the original amorphous region of cast Nafion (10°-16° and 25°-50° of 2θ) for the composite membranes. It is shown that peak positions shift to lower Bragg angle as HA increases in the composite membranes.

Water uptake content

The water absorption content was monitored as a function of time and the water uptake content of composite membranes, calculated by eqn. (5), reduced as the HA increases (Table 3). The cast Nafion membrane undergoes 30% water absorption at r.t, similar to other results [18, 44,47,48] whereas composite membranes displays 16 – 27% water absorption. Certainly, composite membranes have lower water uptake contents than that of cast Nafion. It is thought that there is a strong relationship among crystallinity, water uptake content, and incorporated amount of HA. Assuming that water doesn't exist in the crystalline region, most of water should exist only in the amorphous region and thereby naturally low crystalline material has more water within its structure, which is contrary to high crystalline material. Finally, one reason of the decrease in water uptake content in composite membranes is based on the increase in crystallinity.

Conclusions

In the HA/Nafion composite membranes, it was found that crystallinity increased as HA increases. New crystalline peaks were created in the amorphous region of cast Nafion. It is expected that HA can modify the amorphous structures including cluster region. It is believed that lower water uptake of composite membranes is due to an increase in crystallinity and reduction in free volume owing to embedded HA, which lowers the methanol sorption/desorption diffusivity and suppress methanol crossover in the HA/Nafion composite membranes.

Acknowledgements.

This work was supported by a Grant-in-aid for Scientific Research (No. 13134101) from the Ministry of Education, Science, in Japan.

References

1. Jung, D. H.; Cho, S. Y.; Peck, D. H.; Shin, D. R.; Kim, J. S. J. Power Sources 2002, 173, 106.
2. Yang, B.; Manthiram, A. Electrochem. Comm. 2004, 231, 6.
3. Fujimura, M.; Hashimoto, T.; Kawai, H. Macromolecules 1981, 14, 1309.
4. Yu, C.; Wang, Y.; Hua, K.; Xing, W.; Lu, T. Sensors and Actuators B 2002, 86, 259.
5. Vishnyakoy, A.; Nei,ark, A. J. Phys. Chem. B 2000, 104, 4471.
6. Y. Hsu, W.; Gierke, T. D. J. Membr. Sci. 1983, 13, 307.
7. Schwitzgebel, G.; Endres, F. J. Electroanal. Chem. 1995, 386, 11.
8. Xue, T.; Trent, J. S.; Osseo-Asare, K. J. Membr. Sci. 1989, 45, 261.
9. Gierke, T. D.; Munn, G. E.; Wilson, F. C. J. Polym. Sci., Polym. Phys. Ed. 1981, 19, 1687.
10. Kreuer, K. D. J. Membr. Sci. 2001, 185, 29.
11. Kim, J. W.; Kim, B. K.; Jung, B. S.; J. of Membr. Sci. 2002, 207, 129.
12. Zeng, R.; Pang, Z.; Zhu, H. J. Electroanal. Chem. 2000, 490, 102.
13. Choi, W. C.; Kim, J. D.; Woo, S. I. J. Power Sources 2001, 96, 411.
14. Shao, Z. G.; Wang, X.; Hsing, I. M. J. Membr. Sci. 2002, 210, 147.
15. Sungpet, A. J. Membr. Sci. 2003, 226, 131.
16. Antonucci, P. L.; Arico, A. S.; Creti, P.; Ramunni, E.; Antonucci, V. Solid State Ionics 1999, 125, 431.
17. Shim, J. P.; Ha, H. Y.; Hong, S. A.; Oh, I. H. J. Power Sources 2002, 109, 412.
18. Dimitrova, P.; Friedrich, K. A.; Vogt, B.; Stimming, U. J. Electroanal. chem. 2002, 532, 75.
19. Jung, D. H.; Cho, S. Y.; Peck, D. H.; Shin, D. R.; Kim, J. S. J. Power Sources 2003, 118, 205.
20. Yang, C.; Srinivasan, S.; Bocarsly, A. B.; Tulyani, S.; Benziger, J. B. J. Membr. Sci. 2004, 237, 145.
21. Kim, Y. J.; Choi, W. C.; Seong, I. W.; Hong, W. H. J. Membr. Sci. 2004, 238, 213.

22. Mauritz, K. A.; Payne, J. T. J. Membr. Sci. 2000, 168, 39.
23. Tricoli, V.; Nannetti, F. Electrochim. Acta 2003, 48, 2625.
24. Mauritz, K. A. Material Science and Engineering 1998, 6, 121.
25. Gobinda C, Maiti and Friedemann Freund, 1981, 949.
26. Yamashita, K.; Kitagaki, K.; Umegaki, T. J. Am. Ceram. Soc., 1995, 78, 1191.
27. Yamashita, K,; Owada, H.; Umegaki, T.; Kanazawa, T. Solid State Ionics 1990, 40, 918.
28. Abu B. M. S.; Cheang, P.; Khor, K. A. J. Materials Processing Technology 1999, 89, 462.
29. Yeo, S. C.; Eisenberg, A. J. Appl. Polym. Sci. 1977, 21, 899.
30. Watari, T.; Wang, H.; Kuwahara, K.; Tanaka, K.; Kita, H.; Okamoto, K.I. J. Membr. Sci. 2003, 219, 137.
31. Scigala, R.; Welochowicz, A. Acta Polymerica 1989, 40, 15.
32. Heuvel, H. M.; Huisman, R.; Lind, K.C.J.B. J. Polym. Sci. Polym. Phys. Ed. 1976, 14, 921.
33. Liu, W. J. of Power Sources 1997, 68, 344.
34. Walker, W. J of Power sources 2002, 110, 144.
35. Crank, J.; Park, G.S. Diffusion in Polymers; Academic Press: New York, 1968, 16 and 141.
36. Yeo, C.; Eisenberg, A. J. Appl. Polym. Sci. 1977, 21, 899.
37. Amerongen, G. J. V. Rubber chem. Technol., 1964, 37, 1065.
38. Legras, M.; Hirata, Y.; Nguyen, Q. T.; Langevin, D.; Metayer, M. Desalination 2002, 147, 351.
39. Skou, E.; Kauranen, P., Hentschel, J. Solid State Ionics 1997, 97, 333.
40. Ren, X.; Zawodzinski Jr., T. A.; Uribe, F.; Dai, H.; Gottesfeld, S. In Proc. First int. Symp. Proton Conducting Membrane Fuel Cells, Ed,; Gottesfeld, S.; Halpert, G.; Lsndgrebe, 1995.
41. Springer, T. E.; Zawodzinski, T. A.; Gottesfeld, S. J. Electrochem. Soc. 1991, 138, 2334.
42. Roche, E. J.; Stein, R. S.; Russel, T. P.; Macknight, W. J. J. Polym. Sci. Polym. Phys. Ed. 1980, 18, 1497
43. Nandakumar, P. Material Science and Engineering, 2001, B83, 61.
44. Shao, Z.G.; Joghee, P.; Hsing, I. M. J. Membr. Sci. 2004, 229, 43.
45. Dimitrova, P.; Friedrich, K. A.; Stimming, U.; Vogt, B. Solid State Ionics, 2002, 150, 115.
46. Bakar, M. S. A.; Cheang, P.; Khor, K. A. J. Materials Processing Technology 1999; 89: 462.
47. James, P. J.; Ellott, J. A.; McMaster, T. J.; Hanna, S.; Miles, M. J. J. Material Sci., 2000, 35, 5111.
48. Charles W. Walker Jr., J of Power sources 2002; 110: 144.